Dynamics of an Excess Electron at Metal/Polar Interfaces

Preston T. Snee,[†] Sean Garrett-Roe, and Charles B. Harris*

Department of Chemistry, University of California, Berkeley, California 94720, and Chemical Sciences Division, Ernest Orlando Lawrence Berkeley, National Laboratory, Berkeley, California 94720

Received: December 21, 2002

The low-temperature equilibrium and nonequilibrium solvation dynamics of an excess electron in bulk and at a surface interface have been characterized using mixed quantum/classical simulation methods. A methanol bath was modeled using classical molecular dynamics, whereas the properties of an excess electron were calculated from a wave function based approach. The temperature dependence of the bulk response has been found to be minimal, which may indicate that large scale hydrogen bond breaking and diffusive motion may not play important roles in the solvation dynamics. The equilibrium dynamics have also been compared to nonequilibrium simulations of charge injection into the neat bath. An excess electron at a methanol/Pt(100) surface interface has been shown to become solvated by the bath yet is less bound by a factor of ∼2 compared to the bulk. The solvent response function also displays interesting differences when compared to the low temperature bulk glass. These results also reveal many of the microscopic properties of the solvated interfacial electrons that have recently been observed from ultrafast two photon photoelectron spectroscopy studies.

I. Introduction

One of the most important veins of recent research in chemical physics has been connecting the dynamics of a solvent to perturbations of the local environment. Solvation in bulk systems has received much attention recently, aided by increasingly powerful theoretical molecular dynamics simulations and experimental techniques. In combination, theoretical and experimental studies have been used to assign the various time scales of solvation to characteristic molecular and large scale solvent motions.

Although identified in 1908,[1] the solvation dynamics of the excess electron in bulk liquids is still the subject of numerous experimental[2−7] as well as theoretical[8−11] investigations. Extending the understanding of solvated electron dynamics developed from bulk systems to those of reduced dimensionality is of clear interest given the many processes that occur in quasi-two-dimensional environments, such as electron transfer in electrochemistry and in molecular electronic devices.[12] This is especially true since the recent observation of solvated electrons at low-temperature polar adsorbate/metal surface interfaces from ultrafast two photon photoemission (TPPE) experiments.[13−15] The interfacial bath with which the excess electron interacts may have distinct physical differences from the bulk due to the intrinsic asymmetry of the environment. The interfacial potential may alter the equilibrium structure of an adsorbate layer and hinder certain molecular motions compared to the isotropic bulk.[16−18] To study how the differences in two- or three-dimensional environments affect the properties of solvated electrons, our group has simulated a quantum mechanical electron in a classical methanol bath in low-temperature bulk and at a surface interface. The results have shown that excess electrons reside in a bound, localized potential well in systems with slab geometry despite the change in dimensionality. While the electron is solvated by the interfacial bath, the binding energy and solvation dynamics display interesting differences compared to observations made in a bulk environment.

II. Methods

A. Methanol-Electron Pseudopotential and the Electron Wave Function. As a result of the low mass and large kinetic energy of the particle, simulations involving an excess electron must use theoretical methods firmly based on quantum mechanical principles. Likewise, because of the relatively heavy mass of a solvent molecule such as methanol, a classical description of the bath is sufficient. To conduct mixed quantum classical simulations, all that is needed is a pseudopotential to account for the solute/solvent interactions and a method to solve the Schrödinger wave equation for the excess electron. The coupling of the excess electron to the solvent (i.e., the force the solvent feels from the quantum mechanical particle) may be calculated from the Hellmann−Feynman theorem.[19,20]

In 1993, Zhu and Cukier derived a pseudopotential to describe the energetics of a methanol molecule with an excess electron.[21] Their model potential has the form

$$V(r) = V^{\mathrm{el}}(r) + V^{\mathrm{p}}(r) + V^{\mathrm{r}}(r) + V^{\mathrm{ex}}(r) \qquad (1)$$

in which V^{el} describes the electronic, V^{p} the polarization, V^{r} the repulsion, and V^{ex} the exchange contributions to the total energy of the electron.[22] The variable r is the electron/methanol O, H, or CH_3 site distance. The details of this potential have been discussed in ref 21, and the parameters are summarized in Table 1.

In simulations involving systems with finite periodicity, the size of the (periodically replicated) simulation box requires the use of a spatial cutoff in the evaluation of the potential. This cutoff prevents direct evaluation of the significant long-range Coulombic and polarization interactions of the extended bath with the excess electron. The long-range Coulomb potential has been accounted for by using the Ewald summation technique.[23,24]

* To whom correspondence should be addressed. E-mail: harris@socrates.berkeley.edu.

[†] Present address: MIT, Department of Chemistry, 77 Massachusetts Ave., Cambridge, MA 02139.

10.1021/jp022665o CCC: $25.00
Published on Web 12/04/2003

TABLE 1: Pt(100)/Methanol Potential Parameters

O-Pt(100) :kJ/mol		CH_3−Pt(100):[a] kJ/mol		H−Pt(100):[b] kJ/mol	
A1	60382.3559	A8	3178822.309	A13	8.028
A2	−477.6497	A9	2096.8431	A14	−0.168
A3	238.0177	A10	0.2847446	A15	0.0050
A4	9019.8	A11	12774.97		
A5	−5564.9	A12	−247.209		
A6	−210.8173				
A7	108.8193				

	nm^{-1}		nm^{-1}		nm^{-1}
B1	30.14	B8	48.6752	B13	9.9020
B2	7.6517	B9	15.7219	B14	21.9630
B3	8.0555	B10	0.1245	B15	30.0550
B4	14.8032	B11	22.9003		
B5	13.3941	B12	11.7690		
B6	5.8097				
B7	4.1003				

[a] This potential is derived for a CH_4−Pt(100) potential. [b] From ref 30.

The long range correction of the polarization potential has been estimated from[25]

$$V_{\mathrm{lrc}} = 4\cdot\pi\int_{rc}^{\infty} r^2\, V(r)\, g(r)\, \mathrm{d}r \qquad (2)$$

where *rc* is the cutoff used in the simulations for the potential $V(r)$, which has been set to half of the periodic box length in the present simulations.[26] The long range correction may then be applied via simple analytic integration of eq 2 with the assumption that the radial distribution function has no structure and is equal to unity at large length scales. The correction for the polarization potential in bulk simulations is −0.35 eV for the room-temperature results and −0.43 eV for the glassy bulk simulations. This long range correction for the polarization potential in the surface simulation has been found to be negligible.

The wave function of the excess electron must be calculated once the potential has been defined. The FFT based pseudospectral method of Feit and Stieger has been employed for this purpose and is discussed further in the Supporting Information.[27−29] The pseudospectral method involves the time evolution of a trial wave function on a grid of 16 × 16 × 16 points in 3D space. Once the eigenvalue of the ground state of the Hamiltonian has been determined from the imaginary time dynamics of the trial wave function, the ground-state eigenvector may be calculated. The force that the methanol solvent experiences from the finite charge of the ground-state electron density at each grid point is then determined from the Hellmann−Feynman theorem, and the classical dynamics are integrated for a single time step. This process is repeated at each time step for the length of the simulation.

B. Methanol-Pt(100) Potential. To model the electron/bath system at a 2D surface interface, a potential is needed to describe the interaction of a methanol bath with a metal surface. The present study uses a methodology developed in previous investigations of water on a Pt surface.[30,31] An empirical force field has been derived to fit the results of several density functional theory (DFT) calculations of methanol interacting with a small cluster of platinum atoms. The results are then extended to describe the interactions of a methanol bath with a periodic Pt(100) surface.

The parameters of the methanol−Pt(100) surface potential were fitted to the calculated interaction energies of a single methanol molecule with a cluster of 5 Pt atoms.[32] The LANL2DZ basis set and effective core potential was used for Pt, and the 6-31G** basis set for H, O, and C was used at the B3LYP level of theory.[33−38] These calculations were conducted with the JAGUAR package.[39] The oxygen atom and CH_3 site of the methanol molecule was constrained at various *z* distances over the center, bridge, and top positions of the platinum cluster of 5 atoms while the remaining geometric parameters were optimized. The H−Pt(100) potential of ref 30 was directly employed, and an empirically derived CH_4/Pt(100) potential was calculated using the same methods described above.[40] The CH_4/Pt(100) potential was used to describe the CH_3−Pt(100) interaction. These results were then used to optimize the final methanol−Pt(100) pseudopotential, which takes the following form:

TABLE 2: Simulation Parameters Used for the Solvent and Solvent/Electron Potential

site	q_i/e	$\alpha_I/Å^3$	γ_i	n_i	z_i	$\sigma_{ij}/Å$	ϵ_{ij}/k_b
H	0.431	0.0	0.0	1	0	0.0	0.0
O	−0.728	1.44	0.0	8	0	3.083	87.94
CH_3	0.297	1.7	0.3	6	1	3.861	91.15

$$V = V_{\mathrm{oxy}} + V_{\mathrm{meth}} + V_{\mathrm{h}}$$

where

$$V_{\mathrm{oxy}} = o0 + o1q1 + o2q2$$

$$o0 = \mathrm{A1}\exp(-\mathrm{B1}r_z) + \mathrm{A2}\exp(-\mathrm{B2}r_z) + \mathrm{A3}\exp(-\mathrm{B3}r_z)$$

$$o1 = \mathrm{A4}\exp(-\mathrm{B4}r_z) + \mathrm{A5}\exp(-\mathrm{B5}r_z)$$

$$o2 = \mathrm{A6}\exp(-\mathrm{B6}r_z) + \mathrm{A7}\exp(-\mathrm{B7}r_z)$$

$$V_{\mathrm{meth}} = c0 + c1q1 + c2q2$$

$$c0 = \mathrm{A8}\exp(-\mathrm{B8}r_z) + \mathrm{A9}\exp(-\mathrm{B9}r_z) + \mathrm{A10}\exp(-\mathrm{B10}r_z)$$

$$c1 = \mathrm{A11}\exp(-\mathrm{B11}r_z)$$

$$c2 = \mathrm{A12}\exp(-\mathrm{B12}r_z)$$

$$V_{\mathrm{h}} = h0 + h1q1 + h2q2$$

$$h0 = \mathrm{A13}\exp(-\mathrm{B13}r_z)$$

$$h1 = \mathrm{A14}\exp(-\mathrm{B14}r_z)$$

$$h2 = \mathrm{A15}\exp(-\mathrm{B15}r_z)$$

and

$$q1 = \cos(2\pi r_x/l)\cos(2\pi r_y/l)$$

$$q2 = \cos(4\pi r_x/l) + \cos(4\pi r_y/l)$$

with l = 0.392 nm, the lattice constant of Pt(100). The parameters are given in Table 2. The rms error of this model was found to be 0.9 kcal/mol for the 20 optimized structures used in the fitting.

It was found that the optimal position for the methanol was at the top position of the cluster, which has an interaction energy of −14.6 kcal/mol. The next favorable position was in the center of the four platinum atoms followed by the bridging position by −4.17 and −4.09 kcal/mol, respectively. The [CH_4 or CH_3]/Pt(100) potential is mostly repulsive except at the top position, which has a well depth of −2.57 kcal/mol. The potential energy

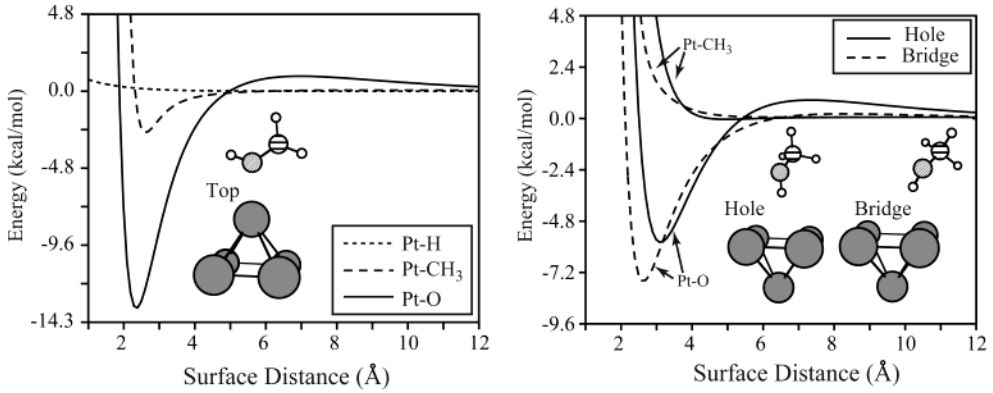

Figure 1. Potential energy surfaces and optimal structures of methanol at various positions on a platinum cluster.

TABLE 3: Simulation Parameters Used in the Various Simulations

bath, temp	time step (fs)	box length (Å)	electron grid size (Å)
bulk, 300 K	5	23.82	0.74
bulk, 100 K	5	22.65	0.74
surface, 100 K	5	35.28[a]	0.85

[a] In the x and y periodic directions.

surfaces for the methanol sites at the top position are shown on the left of Figure 1, and the Pt−O, Pt−H, and Pt−CH_3 potential surfaces are shown on the right. The optimized top, bridge, and hole structures are shown in the insets of Figure 1. These calculated structures and energetics are in agreement with previous experimental and theoretical studies of similar systems.[41,42]

C. Simulation Parameters. The methanol pair interaction is described by the H1 model of Haughney et al., which has been found to adequately represent the bulk properties of the liquid.[43] The Lennard-Jones parameters and electrostatic charges are given in Table 2. Standard molecular dynamics methods have been used to calculate the time evolution of the positions of 200 classical methanol molecules in all of the simulation results presented. The trajectory of the methanol molecules was calculated using the Verlet algorithm,[44,45] while the internal geometry is fixed with the SHAKE method.[46] The time step in all simulations was set to 5 fs. Specific parameters are discussed below and are summarized in Table 3.

Bulk Simulations. The dynamics of an excess electron in a fully periodic methanol bath have been simulated within the NVT ensemble for the equilibrium simulations. The nonequilibrium calculations were performed in the NVE ensemble. The density of methanol was fixed to 0.786 g/cm^3 for the simulations at 300 K and was increased to 0.914 g/cm^3 for the 100 K methanol bath.[47] The excess electron was allowed to equilibrate for a minimum of 50 ps and while properties and response functions were calculated over an additional 75 ps.

As the equilibrium and nonequilibrium properties of the excess electron in room-temperature methanol have been studied previously,[21,48,49] we did not conduct nonequilibrium simulations under these conditions. However, the nonequilibrium response of a low-temperature bath has been investigated. These simulations were performed by allowing the wave function of the excess electron to evolve in an equilibrium configuration of low-temperature bulk methanol that is frozen in position. Once the evolution of the wave function had reached a steady state, the motion of the electron and the bath molecules were allowed to propagate for ∼1.5 ps. The present results are based upon 20 simulations conducted in this manner.

Surface Simulations. The dynamics of an excess electron in a 2D periodic methanol bath have been simulated within the NVT ensemble for the equilibrium simulations. Periodic boundary conditions were enforced in the *x* and *y* directions. To describe the long range Coulombic interactions, the Ewald method has been utilized with a large *z* simulation edge length to minimize layer-to-layer interactions. This approach has been used successfully in several recent investigations of interfacial systems with slab periodicity.[24,50−53] As the split operator method is unstable when divergent potentials are close to the grid edge,[54] a surface image potential was not used in these simulations.[55−59] The *x* and *y* box length was set to 35.28 Å, and the *z* length was set to 3 times this value. Given the lattice constant of Pt(100), this geometry represents approximately 2.5 monolayers of methanol. Our preliminary work showed that the excess electron needed 125 ps of simulation time to equilibrate, after which time the dynamics of this system were characterized for an additional 200 ps. Unfortunately, our methods are not suitable to conduct nonequilibrium simulations under these conditions as discussed below.

As part of the characterization of the electron, we have developed a novel method for calculating radial distribution functions for systems with slab periodicity. The algorithm is based on an "on-the-fly" normalization scheme and does not require any a priori approximation. A full description of our method is given in the Supporting Information section.

III. Results

The purpose of this study is to characterize the equilibrium and nonequilibrium solvent response of low-temperature methanol to an excess electron in the bulk and under 2D conditions. The results have revealed that the both the solvent structure, binding energies and solvation dynamics of the excess electron depend on the dimensionality of the bath. The results of these simulations are discussed in detail below.

A. Room-Temperature Methanol. We have run equilibrium simulations of the solvated electron in room-temperature methanol in order to provide a contrast to the low-temperature bulk data. The results are summarized in Table 4. Shown in Figure 2 are the radial distribution functions of the e^-−H, e^-−O, and e^-−CH_3 site pairs. The results indicate that the electron is preferentially solvated with the electropositive H end of the solvent pointing toward the electron center of mass, as has been observed previously using this model.[21,48] Integration of the radial distribution indicates that there are 4−6 solvent molecules occupying the first solvent shell and there is no indication of long range order, which is consistent with a bulk liquid solution. The equilibrium solvation correlation function

TABLE 4: Average Properties of the Solvated Electron in the Various Simulations Reported

bath, temp	binding energy (eV)	$\langle \delta BE^2 \rangle^{1/2}$ (eV)	potential energy (eV)	kinetic energy (eV)	size[b] (Å)
bulk, 300 K	−1.95[a]	0.28	−3.74[a]	1.79	2.61
bulk, 100 K	−2.33[a]	0.14	−4.32[a]	1.99	2.32
interface, 100 K	−1.12	0.09	−1.98	0.86	3.69

[a] The long range correction factor to the polarization has been applied to these results. [b] Calculated as $\langle \Psi|(r - r_0)^2|\Psi\rangle^{1/2}$, where r_0 is defined as $\langle \Psi|r|\Psi\rangle$.

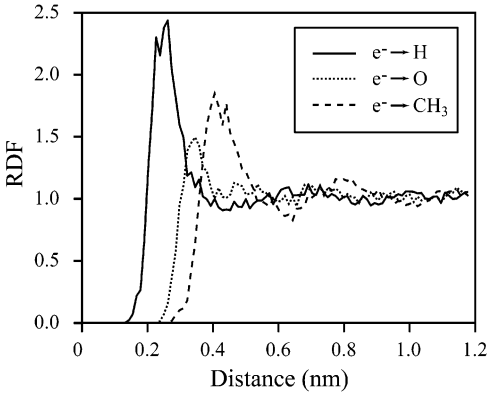

Figure 2. Radial distribution functions of room-temperature bulk methanol with the solvated electron.

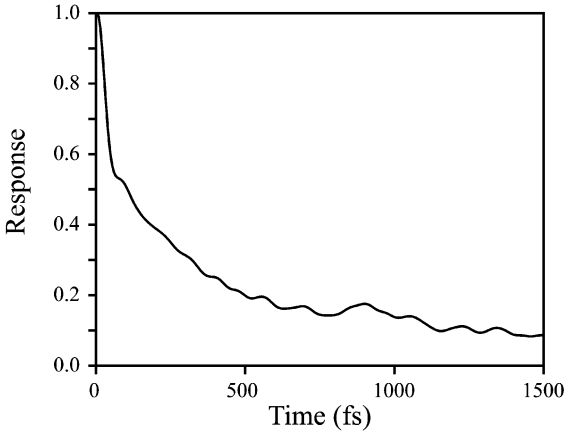

Figure 3. Solvation dynamics of an excess electron in room-temperature bulk methanol.

for the solvated electron is shown in Figure 3. The best fit indicates that there exists an initial 25 fs Gaussian response, followed by biexponential decays of 220 fs and ∼1.7 ps, respectively. Similar results have been reported previously using this model.[49]

B. Low-Temperature Bulk Methanol. The results of the simulations of the excess electron in low temperature bulk methanol reveal several properties of solvation in a glassy medium. For one, the kinetic energy (which is a measure of the size of the solvent cavity of the quantum mechanical electron) increases to 1.99 eV compared to the 1.79 eV value in the room temperature liquid results. This fact is reflected in the change in the radius of gyration of the spherically symmetric ground state, which contracts from 2.6 to 2.3 Å with the decrease in temperature. The compression of the electron and the larger kinetic energy are likely the result of the increased ordering of the solvent structure about the excess electron at low temperatures, as shown in the radial distribution functions in Figure 4. This enhanced local structure of methanol about the electron

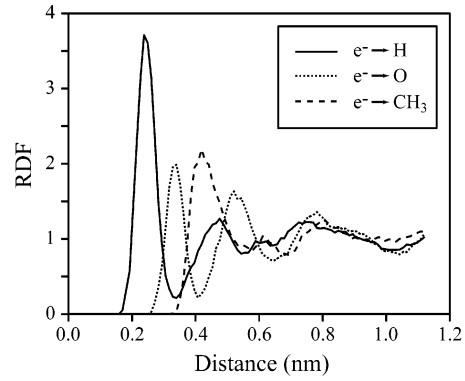

Figure 4. Radial distribution functions of frozen bulk methanol glass with the solvated electron.

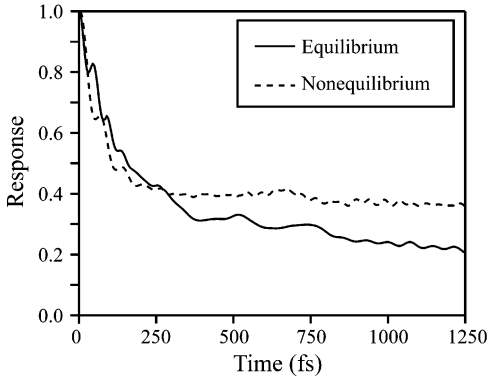

Figure 5. Equilibrium (solid line) and nonequilibrium (dashed line) solvation dynamics of an excess electron in frozen bulk methanol glass.

is indicative of more favorable solvent interactions with the particle, which is reflected by the lowering of the binding energy by −0.38 eV in the low temperature glass compared to the ambient liquid. Integration of the radial distribution functions indicates that 4 methanol molecules comprise the first solvent shell. Overall, the electron is much more strongly bound in the frozen glass compared to the electron at room-temperature solution.

Shown in Figure 5 are the equilibrium and nonequilibrium solvation dynamics of the excess electron in frozen methanol glass. The best fit to the equilibrium solvation dynamics is composed of a 22 fs Gaussian response and a 87 fs followed by a ∼1.6 ps exponential decay.[60] The ps bath response in low-temperature methanol glass is similar to the long time exponential decay in the room-temperature liquid, which is surprising given that long time scale exponential solvation dynamics are often the result of diffusive bath motion.

The nonequilibrium dynamics of electron injection into the low-temperature methanol glass have also been simulated. As has been observed in previous room-temperature charge injection studies,[49] the electron probability distribution is initially diffuse and quickly collapses. There is a corresponding fast increase in the kinetic energy which then relaxes by ∼0.4 eV. As shown in the inset of Figure 6, the electron initially has 4 methanol molecules occupying the first solvent shell which decreases to 1 solvent molecule within ∼200 fs. This process is likely facilitated by the large temperature increase in the first shell to ∼350 K. The population within this shell appears to slowly recover on a time scale much longer than the nonequilibrium trajectory of 1.5 ps.

C. Solvation Dynamics at the MeOH−Pt(100) Interface. The properties and dynamics of an excess electron at a surface interface have also been investigated. As shown in the *z*-

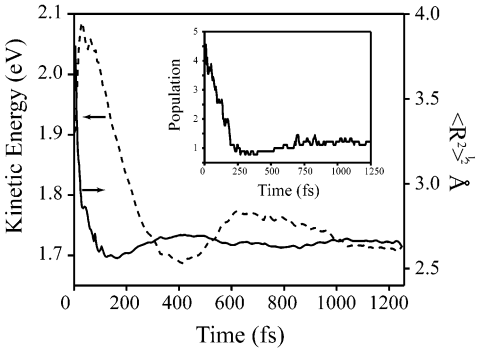

Figure 6. Properties of the electron and bath during the nonequilibrium charge injection into low-temperature bulk methanol. The dashed line represents the kinetic energy, whereas the solid line represents the radius of gyration of the excess electron. The inset shows the population in the first solvent shell.

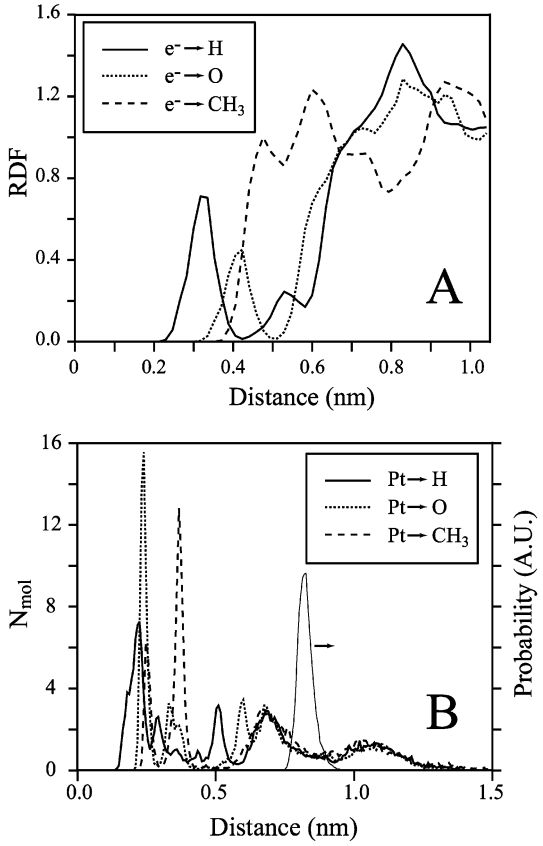

Figure 7. A. Radial distribution functions of methanol with the solvated electron at a Pt(100) surface interface. The method that was used to calculate these data is discussed in the Supporting Information section. Also shown in B are the *z*-dependent distributions of the methanol H, O, and CH_3 sites and electron probability amplitude, with the metal surface defined to be at the origin.

dependent distribution functions of Figure 7B, the methanol bath has an ordered first layer interacting with the surface, whereas the second and third layers are more amorphous. The probability distribution of the electron expectation value in the *z* direction is sharply peaked ~0.9 nm placing the electron primarily between the second and third layers. Overall, the loss of dimensionality in a single direction results in the electron becoming less bound at the surface interface by a factor of ~2 compared to in the low temperature bulk. There is a corresponding decrease in the kinetic energy and expansion of the radius of gyration of the excess electron. The extra spatial width of the electron also manifests itself in the 2D radial distribution

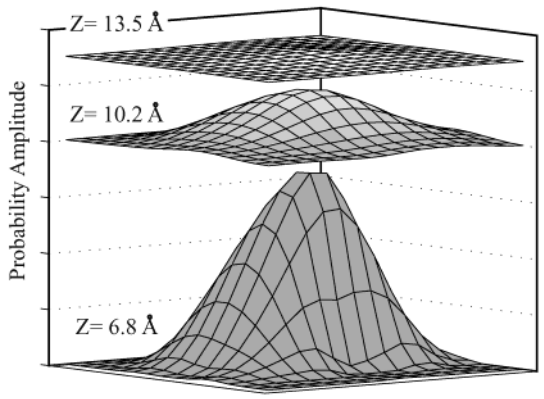

Figure 8. Probability amplitude of an equilibrated electron wave function from a single interfacial configuration. The *z* distances correspond to the height from the bottom of the electron's configurational grid. Each grid spacing is 0.85 Å in length.

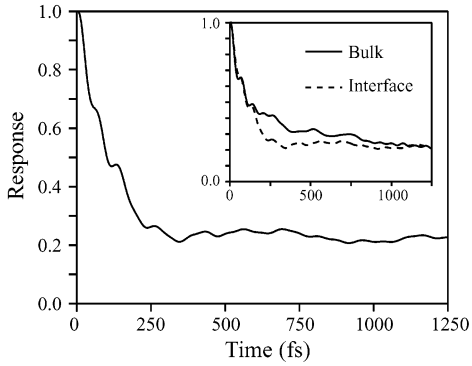

Figure 9. Equilibrium solvation dynamics of an excess electron in a low-temperature methanol/Pt(100) surface interface. The interfacial dynamics appear biphasic rather than triphasic like the bulk response (inset).

functions shown in Figure 7A, for which the closest approach for the hydrogen and oxygen sites are nearly 1 Å greater than observed in bulk simulations. These results also indicate that there is a significant change in the solvent structure for the interface, with the CH_3 site distribution almost overlapping and dominating over that of the oxygen site. Nonetheless, as shown in Figure 8, the electron has the greatest probability amplitude at the center of the configurational grid and does not have significant amplitude at the boundaries, indicative of a solvated state for the electron.

Shown in Figure 9 is the interfacial solvent response function. The equilibrium response can be best described by a two component decay of 100 fs followed by a long time scale component of several picoseconds.[60,61] Despite repeated attempts, the nonequilibrium calculations could not be performed as the split operator method did not converge to a localized wave function in the initial step. Consequently, the FFT grid based algorithm gives spurious results and the subsequent simulation is not a reliable representation of the dynamics of the system.

IV. Discussion

A. Bulk Results. Structure and Dynamics. The structure of the solvated electron in the frozen bulk shows that the electron is stabilized under glassy conditions relative to the room-temperature liquid. The nearest location of the H site of the solvent compresses to within 2.4 Å and slightly overlaps the wave function of the electron, which has a radius of gyration

TABLE 5: Time Scales and Weights of the Three Component Equilibrium Solvation Dynamics Observed in Bulk Systems

bath, temp	Gaussian component, fs	exponential decay, fs	exponential decay,[a] ps
bulk, 300 K	25 (33%)	220 (45%)	1.7 (22%)
bulk, 100 K	22 (15%)	87 (42%)	1.6 (43%)

[a] The long time decay is difficult to fit due to insufficient sampling. While the absolute values of the decay constants are not certain, they are of the same order of magnitude.

of 2.3 Å in low-temperature methanol glass. Integration of the radial distribution functions reveals that 4 methanol molecules comprise the first solvent shell. These results are in excellent agreement with the earlier ESR studies by Kevan.[62,63] Those investigations found that excess electrons prepared by ionizing radiation in 1.5 K methanol glass were solvated by 4 molecules with an average electron/proton distance of 2.3 Å.

The equilibrium solvation dynamics of the excess electron in glassy low temperature methanol are similar to those observed in the room temperature liquid. The solvation dynamics under ambient and low temperature conditions are best fit by three components, an initial Gaussian followed by two exponential decays. As shown in Table 5, the fast Gaussian component is more important in the room temperature liquid, whereas the long time scale exponential is the dominant contribution to the dynamics in the low temperature glass. While the relative importance of the dynamical motion for solvation depends on the temperature of the bath, the solvation time scales are largely identical. Thus, if the Gaussian and fast exponential components are due to reorientation of the solvent OH bonds, then the overall hydrogen bond network must not be significantly perturbed as the resulting dynamic would be much slower in the low-temperature glass. Likewise, the fact that the long time scale decays are similar at room temperature and at 100 K is not consistent with solvent or solute diffusional motion. These observations are identical to the conclusions based on previous studies of electron solvation dynamics in low-temperature glassy media. Low-temperature experiments in alcohols have shown that hydrogen bond breakage is not the limiting factor in the dynamics of electron solvation.[64] These experiments also determined that viscosity does not dominate the solvation process as excess electrons are fully solvated at room temperature and at 77 K.[64,65] These previous reports concluded that molecular reorientation is the dominant solvation process and occurs in both room temperature and low temperature (>77 K) alcohol baths,[64−68] although more recent investigations in room-temperature alcohol solution have concluded that hydrogen bond breaking does occur.[69−72] If large scale hydrogen bond rearrangement is important in electron solvation, then it may be true that we cannot simulate this system for long enough at low temperatures to observe those dynamics in both the equilibrium and nonequilibrium simulations.

The nonequilibrium response of the system to charge injection has been investigated. Shown in Figure 5 are the equilibrium and nonequilibrium response functions to electron solvation, averaged over 20 nonequilibrium simulations. For the most part, the solvent responses appear similar except for the fact that the decay to equilibrium appears to take longer in the charge injection simulations. Shown in Figure 6 are various time dependent properties of the nonequilibrium dynamics. Following charge injection, the kinetic energy initially increases and then rapidly decays, which is mirrored by a fast radial collapse of the electron wave function. This process is accompanied by a loss of population within the first solvent shell from the initial equilibrium value of 4 methanol molecules to ∼1 within 200 fs. The loss of the first solvent shell molecules is likely facilitated by the large increase in the local temperature from 100 to ∼350 K. The first solvent shell population does not appear to recover on the 1.25 ps time scale that these simulations were conducted and likely accounts for the long time scale for the return to equilibrium. This fact is reflected in the kinetic energy and radius of gyration of the electron, neither of which appear to approach their equilibrium values. These observations suggest that the long time scale component to the nonequilibrium dynamics is due to either solvent reorientation or diffusion into the first solvent shell followed by a radial collapse and increase in kinetic energy of the excess electron wave function. It is interesting to note that our findings in low-temperature glass are similar to those reported by Turi et al. in their nonequilibrium room-temperature liquid methanol simulations.[49] This leads us to conclude that both equilibrium and nonequilibrium solvation dynamics do not have substantial temperature dependence.

The dynamics observed in these low temperature charge injection studies are in agreement with experimental findings. Previous results have shown that immediately following charge injection an electron in low-temperature alcohol glasses has absorptions that are red-shifted relative to the equilibrium spectrum.[64,65,71] The present findings suggest that the red shifted spectrum of the solvated electron following charge injection is a result of the destabilization of the ground-state energy level with respect to the first excited states. This is a result of the loss of solvent molecules within the first solvent shell and increase of the radius of gyration of the electron, which has been shown to reduce the ground and excited-state splittings.[41,65] In the language of refs 72−74, in this state, this species may correspond to the weakly bound electron in its ground electronic state, the spectra of which has been proposed to blue shift before the species becomes strongly bound by the solvent.

B. Surface Interface Results. Structure and Dynamics. Recent reports have shown that excess electrons are solvated within a layer of polar molecules deposited on the surfaces of metals.[13−15] To theoretically describe the microscopic properties and dynamics of the excess electron in these systems, we have simulated a quantum mechanical electron trapped in a finite interfacial layer of methanol on a platinum interface.

The results of the present calculations agree with the recent observation of localized solvated electrons in femtosecond two photon photoemission studies at metal interfaces.[13−15] Shown in Figure 8 are the probability amplitudes of the electron's ground-state wave function from a single equilibrated methanol/Pt(100) configuration. The electronic wave function is spherical in shape and localized in character, indicating that the interfacial methanol bath has formed a stable potential trap around the excess electron. It is interesting to note that nonequilibrium simulations were divergent due to the inability to converge the initial wave function to a localized state. This agrees with recent experimental results which found that the excess electron is initially delocalized parallel to an alcohol/Ag(111) surface following charge injection.[13] The spatial extent of the delocalized state estimated in these studies is much larger than could be adequately simulated using available computational resources.

Although these results show that an electron may become solvated by an interfacial bath, the Pt(100) surface provides a markedly different environment for the interaction of the excess electron with the solvent molecules. The interfacial potential alters the solvent structure which in turn affects the electron/methanol interactions. This fact is reflected in the first solvent shell structure. Shown in Figure 7A are the radial distribution

functions of the solvent with the excess electron. Although the electron is largely solvated by the H and O sites, the methyl group almost overlaps the oxygen site and therefore must interact with the electron to a greater extent than in the bulk simulations. The first solvent shell is expanded with respect to the low temperature bulk, which is reflected by the increase of the radius of gyration of the interfacial electron. Although the present findings indicate that the solvated interfacial electron has an uncharacteristically large spatial extent, these results qualitatively agree with recent TPPE studies of nitriles adsorbed on a Ag-(111) surface.[14]

The binding, potential, and kinetic energies are reduced by over a factor of half compared to the results observed in bulk simulations. As discussed above, the loss of binding energy is likely due in part to changes in the interfacial solvent structure and asymmetry in the nonperiodic direction as shown in Figure 7B. The excess electron primarily resides between the second and third methanol layer, as the first layer is held rigid by the strong interactions with the surface edge. Consequently, the reduced fluidity hinders the bath molecules' ability to interact with the excess electron, which becomes less bound as a result. The lack of long range interactions that are significant in the bulk also serves to destabilize the electron. Although both ambient and low temperature methanol have similar three component equilibrium solvent response functions, the dynamics observed at the low temperature surface interface are only biphasic. This point is highlighted in the inset of Figure 9, which shows the overlap of the solvent response in the glassy bulk and at the interface. Consequently, the 2-dimensional bath has less dynamical modes by which it can respond to fluctuations in the solute as are present in the 3-dimensional bulk.

Recent TPPE studies have shown multiphasic femtosecond to picosecond solvent response following charge injection into a polar adsorbate layer.[13−15] This fact is mirrored in our results; however, the differences in the chemical identities of the interfacial systems and our inability to perform nonequilibrium delocalized simulations prevents quantitative agreement with the experimental results. In the future, these simulations will be extended to nitrile and water adsorbates that have been studied experimentally, as well as the adsorbate coverage dependence of the electron dynamics.

V. Conclusion

The structure and dynamics of the solvated electron in low temperature glassy methanol has been shown to agree with the experimental results. The time scales for the solvation dynamics are similar in room temperature and glassy bulk methanol, leading us to conclude that neither large scale hydrogen bond breaking nor diffusional dynamics are responsible for solvation of the excess electron. However, the lack of any observable large scale hydrogen bond or diffusional dynamics may be due to the fact that we cannot perform simulations for long enough to describe such slow processes at low temperatures. The charge injection studies have shown that the loss of solvent population and expansion of the electronic wave function within the first shell is the likely source of the previously observed red-shifted absorptions in low-temperature alcohol solvents.

The simulations of the excess electron at a low-temperature surface has shown that the excess electron is solvated, however destabilized, at the Pt(100)/methanol interface. The loss of binding energy is the result of the interfacial "freezing" of the first bath layer and the lack of long-range polarization interactions. The structure of the excess electron is also altered at the interface, becoming more diffuse which is accompanied by an increase in the size of the solvent cage. The solvation dynamics have been shown to be biphasic, which is in contrast to the dynamics observed in both ambient and room-temperature bulk.

Acknowledgment. We would like to thank the Director, Office of Science, Office of Basic Energy Science, Chemical Sciences Division, under U.S. Department of Energy contract DE-AC03-76SF00098 for support. Also we thank Dr. P. Geissler for helpful discussions concerning Ewald sums. We also acknowledge helpful conversations with Profs. R. Cukier, L. Turi, and P. J. Rossky concerning the electron−methanol pseudopotential.

Supporting Information Available: The method for calculating normalized radial distribution functions of systems with slab geometry. Also details of the quantum dynamics calculations. This material is available free of charge via the Internet from http://pubs.acs.org.

References and Notes

(1) Kraus, C. A. *J. Am. Chem. Soc.* **1908**, *30*, 1323.
(2) Mingus, A.; Gauduel, Y.; Martin, J. L.; Antonetti, A. *Phys. Rev. Lett*. **1987**, *58*, 1559.
(3) Silva, C.; Walhout, P. K.; Yokoyama, K.; Barbara, P. F. *Phys. Rev. Lett.* **1998**, *80*, 1086.
(4) Kloepfer, J. A.; Vilchiz, V. H.; Lenchenkov, V. A.; Bradforth, S. E. *Chem. Phys. Lett.* **1998**, *298*, 120.
(5) de Boeij, W. P.; Pshenichnikov, M. S.; Wiersma, D. A. *Annu. Rev. Phys. Chem*. **1998**, *49*, 99.
(6) Martini, I. B.; Barthel, E. R.; Schwartz, B. J. *Science* **2001**, *293*, 462.
(7) Tauber, M.; Mathies, R. A. *J. Phys. Chem. A* **2001**, *105*, 10952.
(8) Fueki, K.; Feng, D.-F.; Kevan, L. *J. Phys. Chem*. **1970**, *74*, 1976.
(9) Jonah, C. D.; Romero, C.; Rahman, A. *Chem. Phys. Lett.* **1986**, *123*, 209.
(10) Schnitker, J.; Motakabbir, K.; Rossky, P. J.; Friesner, R. *Phys. Rev. Lett*. **1988**, *60*, 456.
(11) Rossky, P. J.; Schnitker, J. *J. Phys. Chem.* **1988**, *92*, 4277.
(12) Villegas, I.; Weaver, M. J. *J. Phys. Chem. B* **1997**, *101*, 10166.
(13) Liu, S. H.; Miller, A. D.; Gaffney, K. J.; Szymanski, P.; Garrett-Roe, S.; Bezel, I.; Harris, C. B. *J. Phys. Chem. B* **2002**, *106*, 7636.
(14) Miller, A. D.; Bezel, I.; Gaffney, K. J.; Garrett-Roe, S.; Liu, S. H.; Szymanski, P.; Harris, C. B. *Science* **2002**, *297*, 1163.
(15) Gahl, C.; Bovensiepen, U.; Frischkorn, C.; Wolf, M. *Phys. Rev. Lett.* **2002**, *89*, 107402.
(16) Benderskii, A. V.; Eisenthal, K. B. *J. Phys. Chem. A* **2002**, *106*, 7482.
(17) Baldelli, S.; Mailhot, G.; Ross, P. N.; Shen, Y. R.; Somorjai, G. A. *J. Phys. Chem. B* **2001**, *105*, 654.
(18) Faeder, J.; Ladanyi, B. M. *J. Phys. Chem. B* **2001**, *105*, 11148.
(19) Feynman, R. P. *Phys. Rev.* **1939**, *81*, 385.
(20) Hellman, H. in *Einfuhrung in die Quantunchemie*; Franz Deuticke: Leipzig, 1937.
(21) Zhu, J. J.; Cukier, R. I. *J. Chem. Phys*. **1993**, *98*, 5679.
(22) The exchange potential of ref 21 should read as $V^{ex}(r) = -\gamma\, e^2/a_o[(3/p)\, r(r)]^{1/3}$.
(23) Ewald, P. *Ann. Phys.* **1921**, *64*, 253.
(24) The use of the Ewald summation technique for ionic systems has been criticized for its artificial periodicity and a few other artifacts which arise using this method. See ref 75.
(25) Allen, M. P.; Tildesley, M. P. *Computer Simulations of Liquids*; Clarendon Press: Oxford, U.K., 1987.
(26) There does not exist a symmetry factor of 1/2 in the evaluation of this long range correction factor.
(27) Feit, M. D.; Fleck, J. A.; Steiger, A. *J. Comput. Phys*. **1982**, *47*, 412.
(28) Feit, M. D.; Fleck, J. A. *J. Chem. Phys.* **1983**, *78*, 301.
(29) Feit, M. D.; Fleck, J. A. *J. Chem. Phys.* **1984**, *78*, 2578.
(30) Foster, K.; Raghavan, K.; Berkowitz, M. *Chem. Phys. Lett*. **1989**, *162*, 32.
(31) Raghavan, K.; Foster, K.; Berkowitz, M. *Chem. Phys. Lett*. **1991**, *177*, 426.
(32) The optimized geometry of 5 Pt atoms in a singlet spin state has been used throughout the present study. Although a cluster of 5 Pt atoms has a septuplet ground state at the present level of theory, the singlet state has the greatest interaction with a methanol molecule.

(33) Hehre, W. J.; Ditchfield, R.; Pople, J. A. *J. Chem. Phys*. **1972**, *56*, 2257.
(34) Hay, P. J.; Wadt, W. R. *J. Chem. Phys*. **1985**, *82*, 270.
(35) Hay, P. J.; Wadt, W. R. *J. Chem. Phys*. **1985**, *82*, 284.
(36) Hay, P. J.; Wadt, W. R. *J. Chem. Phys*. **1985**, *82*, 299.
(37) Becke, A. D. *J. Chem. Phys*. **1993**, *98*, 5648.
(38) Lee, C.; Yang, W.; Parr, R. G. *Phys. Rev*. **1998**, *B41*, 785.
(39) *Jaguar 3.5*; Schrodinger, Inc.: Portland, OR, 1998.
(40) The CH_4/Pt(100) potential interaction was described by optimizing the geometries of several configurations of CH_4 at the top, center and bridging sites of the optimized singlet platinum cluster. A total of nine structures were used in the fitting with an rms error of 0.11 kcal/mol for the reported potential.
(41) Sexton, B. A.; Huges, A. E. *Surf. Sci.* **1984**, *140*, 227.
(42) Greeley, J.; Mavrikakis, M. *J. Am. Chem. Soc.* **2002**, *124*, 7193.
(43) Haughney, M.; Ferrario, M.; McDonald, I. R. *J. Phys. Chem*. **1987**, *91*, 4934.
(44) Verlet, L. *Phys. Rev.* **1967**, *159*, 98.
(45) Hockney, R. W. *Methods Comput. Phys*. **1970**, *9*, 136.
(46) Ryckaert, J. P.; Ciccotti, J. P.; Berendsen, H. J. C. *J. Comput. Phys*. **1977**, *23*, 327.
(47) Sindzingre, P.; Klein, M. L. *J. Chem. Phys.* **1992**, *96*, 4681.
(48) Turi, L.; Mosyak, A.; Rossky, P. J. *J. Chem. Phys*. **1997**, *107*, 1970.
(49) Turi, L.; Minary, P.; Rossky, P. J. *Chem. Phys. Lett*. **2000**, *316*, 465.
(50) Yeh, I.-C.; Berkowitz, M. L. *J. Chem. Phys.* **1999**, *111*, 3155.
(51) Shelley, J. C.; Patey, G. N. *Mol. Phys*. **1996**, *88*, 385.
(52) Alejandre, J.; Tildesley, D. J.; Chapela, G. A. *J. Chem. Phys*. **1995**, *102*, 4574.
(53) Shelley, J. C.; Patey, G. N.; Berard, D. R.; Torrie, G. M. *J. Chem. Phys.* **1997**, *107*, 2122.
(54) Neuhasuer, D.; Baer, M. *J. Chem. Phys*. **1989**, *90*, 4351.
(55) Grimes, C. C.; Brown, T. R. *Phys. Chem. Lett*. **1974**, *32*, 280.
(56) Johnson, P. D.; Smith, N. V. *Phys. Rev. B* **1983**, *27*, 2527.
(57) Dose, V.; Altmann, W.; Goldmann, A.; Kolac, U.; Rogozik, J. *Phys. Rev. Lett.* **1984**, *52*, 1919.
(58) Straub, D.; Himpsel, F. J. *Phys. Rev. Lett*. **1984**, *52*, 1922.
(59) Previous TPPE studies have shown that only a single metal-substrate decoupled electronic state is observed when the surface is coated with multiple layers of methanol.[13] Consequently, we have not included an image potential in these simulations as these results have shown that the excess electron is effectively screened from the metal surface at high coverage.
(60) It is difficult to ascertain the absolute length of the response due to insufficient statistical sampling.
(61) It is difficult to unambiguously fit the shortest time scale equilibrium response to either Gaussian or exponential dynamics. Using either functional form gives short time scale components on the order of 100 fs.
(62) Kevan, L. *Chem. Phys. Lett*. **1979**, *66*, 578.
(63) Kevan, L. *Acc. Chem. Res*. **1981**, *14*, 138.
(64) Chase, W. J.; Hunt, J. W. *J. Phys. Chem*. **1975**, *79*, 2835.
(65) Kevan, L. *J. Chem. Phys*. **1972**, *56*, 838.
(66) Richards, J. T.; Thomas, J. K. *J. Chem. Phys*. **1970**, *53*, 218.
(67) Higashimura, T.; Noda, M.; Warashina, T.; Yoshida, H. *J. Chem. Phys*. **1970**, *53*, 1152.
(68) Hase, H.; Noda, M.; Higashimura, T. *J. Chem. Phys*. **1971**, *54*, 2975.
(69) Hirata, Y.; Mataga, N. *J. Phys. Chem.* **1991**, *95*, 9067.
(70) Fueki, K.; Feng, D.-F.; Kevan, L.; Christoffersen, R. E. *J. Phys. Chem*. **1971**, *75*, 2297.
(71) Baxendale, J. H.; Wardman, P. *J. Chem. Soc., Faraday Trans. 1* **1973**, *69*, 584.
(72) Pepin, C.; Goulet, T.; Houde, D.; Jay-Gerin, J.-P. *J. Phys. Chem.* **1994**, *98*, 7009.
(73) Pepin, C.; Goulet, T.; Houde, D.; Jay-Gerin, J.-P. *J. Chim. Phys.* **1996**, *93*, 182.
(74) Jay-Gerin, J.-P. *Can. J. Chem*. **1997**, *75*, 1310.
(75) Hunenberger, P. H.; McCammon, J. A. *J. Chem. Phys.* **1999**, *110*, 1856.